Spatial field reconstruction with INLA: Application to simulated galaxies

Majda Smole[1], João Rino-Silvestre[2], Santiago González-Gaitán[2], Marko Stalevski[1,3]

1 Astronomical Observatory, Belgrade, Serbia; 2 CENTRA, Instituto Superior Técnico, Lisboa, Portugal; 3 Sterrenkundig Observatorium, Gent, Belgium

14th SCSLSA 2023

19 - 23 June
Bajina Bašta, Serbia

Post-processing technique for MCRT output

- **SKIRT** - MCRT (Monte Carlo Radiative Transfer) code used for simulating radiation transfer in dusty astrophysical systems (Baes & Camps 2015; Camps & Baes 2015). `http://www.skirt.ugent.be`
- **INLA** - Integrated nested Laplace approximation (Rue et al. 2009) is a computational method for approximate Bayesian inference of Latent Gaussian fields
- **R-INLA** - package designed for modeling spatial data (Rue et al. 2017)
- **SKIRT Auriga project** - `https://www.auriga.ugent.be/Home--SKIRT-Auriga-Project.html` synthetic UV-submm images of 30 simulated Milky Way type galaxies (Kapoor et al. 2021)

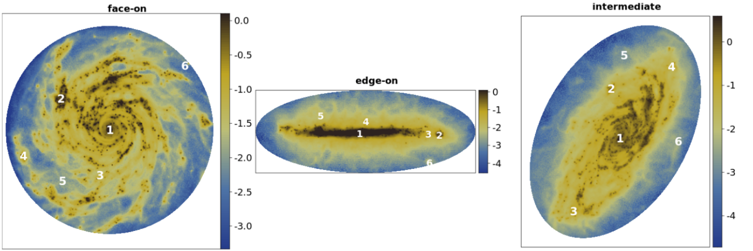

Fig. 1: HPN reference images of Au-16 galaxy at λ = 7.88 μm, viewed at 'face-on' (right), 'edge-on' (middle) and 'intermediate' (right) angle. Colour indicates flux density in MJy/sr , given in logarithmic scale. Numbers on spatial maps indicate positions of pixels whose SEDs are shown in section 3.2.1

Method

- We explore the potential of INLA method as a tool for enhancing the MCRT images

  high photon number (HPN) reference images - 3×10^{10} photon packages SKIRT Auriga images

  low photon number (LPN) input images - 3×10^{8} or 3×10^{9} photon packages

  LPN input images require only few % of the HPN reference simulation execution time

  LPN input image + INLA $\Rightarrow$ HPN reference image

- INLA reconstructions are also time costly! How to reduce INLA reconstruction time?
  1. **Data sampling** - using a percentage of the original data cube as INLA input
  2. **Dimensionality reduction techniques**
     - **PCA** - Principal Component Analysis; **prcomp** R function
     - **NMF** - Non-Negative Matrix Factorization; **nmf** function in R

LPN input + PCA/NMF + INLA $\Rightarrow$ HPN reference

(this work: Smole et al. 2022)

LPN input + AE NN + INLA $\Rightarrow$ HPN reference

(Rino-Silvestre et al. 2022)

Optimal sampling percentage and number of PCA/NMF components - cut 600x600x50

The quality of INLA reconstructions (X'), compared to HPN reference images (X), is quantified by the normalized residuals, calculated as:

$$Residuals\ (\%) = |\frac{X' - X}{X}| \times 100\% \tag{1}$$

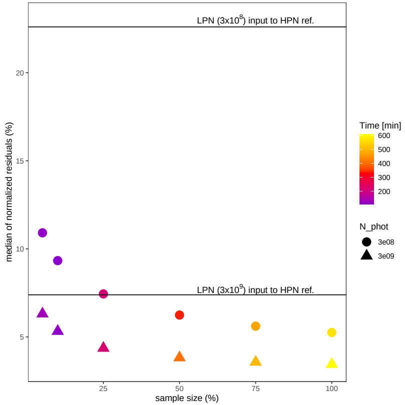

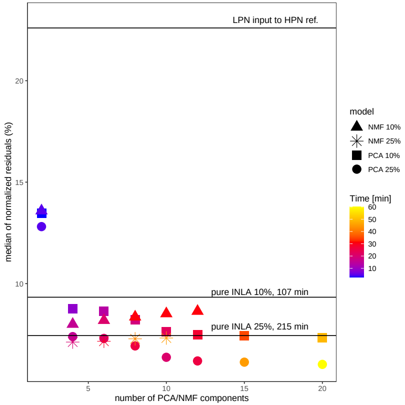

Integrated SEDs

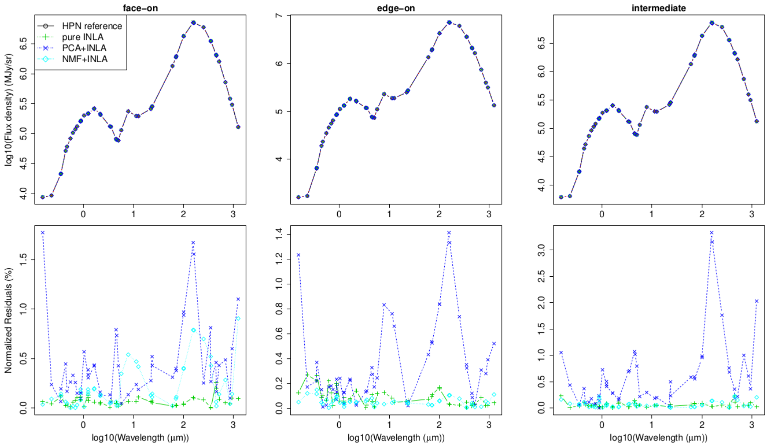

Figure: Integrated SEDs for HPN reference, pure INLA and PCA/NMF+INLA reconstructions (upper panels) with the associated residuals (lower panels), for face-on (left), edge-on (middle) and intermediate (right) cubes.

Single spaxel SEDs - face-on

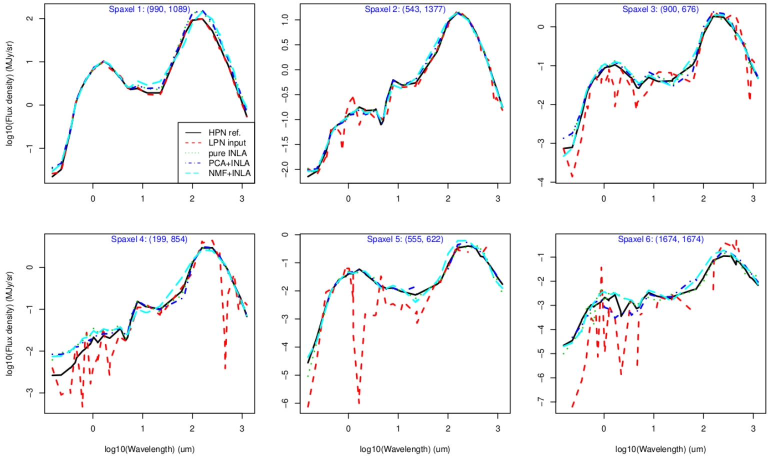

Figure: Single spaxel SEDs for HPN reference (black) and LPN input (red) face-on cubes, together with pure INLA (green) and PCA/NMF+INLA (blue and cyan) reconstructions.

Spatial reconstructions of the face-on cube

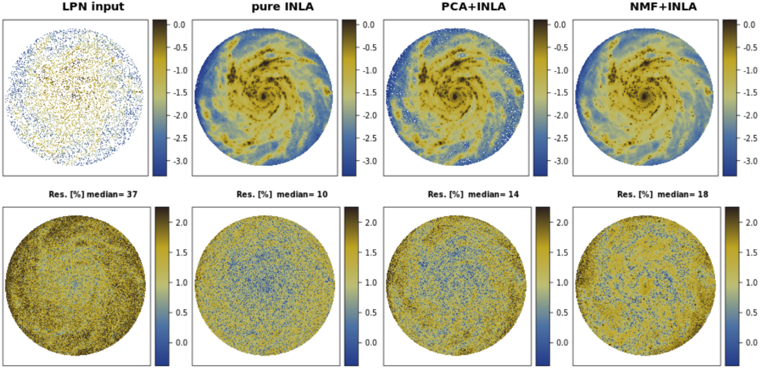

Figure: Spatial reconstructions (upper panels) with the associated residuals (bottom panels) at wavelength bin 7.88 μm. Sample size: 25%, face-on cube.

Spatial reconstructions of the face-on cube

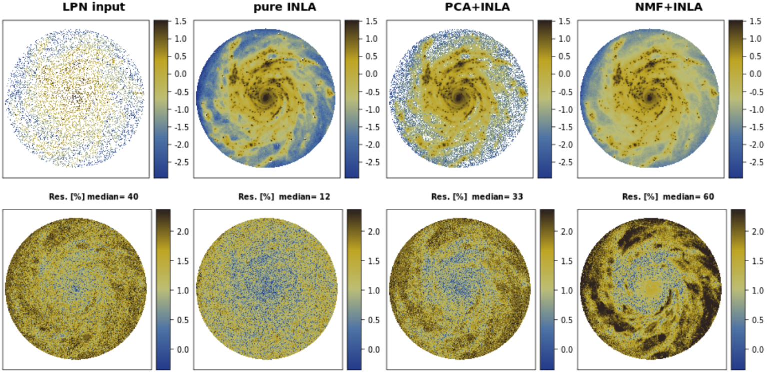

Figure: Spatial reconstructions (upper panels) with the associated residuals (bottom panels) at wavelength bin 100.80 μm. Sample size: 25%, face-on cube.

Spatial reconstructions of the face-on cube

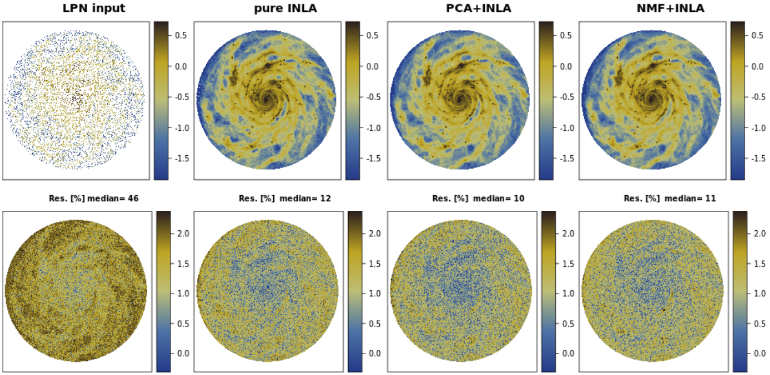

Figure: Spatial reconstructions (upper panels) with the associated residuals (bottom panels) at wavelength bin 515.36 μm. Sample size: 25%, face-on cube.

Spatial reconstructions of the edge-on cube

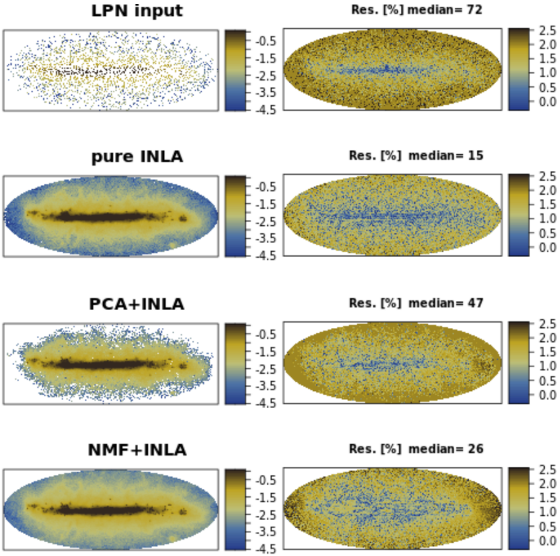

Figure: Edge-on cube at wavelength bin 7.88 μm.

Spatial reconstructions of the intermediate cube

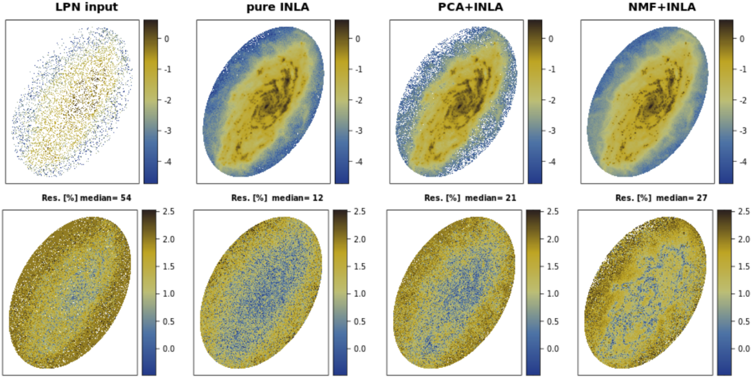

Fig. 13: 'Intermediate' cube at wavelength bin 7.88 μm

Figure: Intermediate cube at wavelength bin 7.88 μm.

Summary

Median of the normalized residuals and the running times for each realization, compared to HPN reference.

angle	photon number	LPN input median (%)	input sample	pure INLA median (%)	pure INLA time (%)	PCA+INLA median (%)	PCA+INLA time (%)	NMF+INLA median (%)	NMF+INLA time (%)
face-on	3×10^9	17.68	25%	9.97	110	10.68	32	11.35	40
			10%	11.61	89	12.21	26	12.79	35
	3×10^8	60.97	25%	15.57	103	15.46	27	17.65	24
			10%	19.22	74	18.20	15	20.00	19
edge-on	3×10^9	30.23	25%	13.36	58	20.62	18	15.85	24
			10%	15.67	43	22.54	15	17.5	20
	3×10^8	96.88	25%	23.42	47	31.18	10	24.92	12
			10%	29.38	28	35.28	7	27.47	8
inter-mediate	3×10^9	24.91	25%	12.10	97	12.63	24	12.73	33
			10%	14.57	76	14.41	21	14.51	26
	3×10^8	86.13	25%	20.03	89	19.27	22	23.00	22
			10%	25.10	66	22.63	13	25.89	16

$$t\ (\%) = \frac{t_{\mathrm{LPN\ SKIRT}} + t_{\mathrm{INLA}}}{t_{\mathrm{HPN\ SKIRT}}} * 100, \quad (2)$$

Conclusions

- Spatially integrated SED closely follow the reference SED for each of the employed methods, with median of the normalized residuals $< 0.3\%$
- Spatial modelling - faint galaxy outskirts have the highest residuals
- Our method offers time-efficient reconstructions
  spatal residuals $\sim 10 - 30\%$ requiring $\sim 7 - 40\%$ of the HPN reference running time
- Optimized LPN simulations can help narrow down the parameters to then run a full HPN simulation.

Smole M., Rino-Silvestre J., González-Gaitán S., Stalevski M., 2022, A&A, 669, 152

References

- Baes M. & Camps P., 2015, Astronomy and Computing, 12, 33
- Camps P & Baes M., 2015, Astronomy and Computing, 9, 20
- Kapoor A. U., Camps P., Baes M., et al. 2021, MNRAS, 506, 5703
- Rino-Silvestre J., González-Gaitán S., Stalevski M., et al. 2022, Neural Computing and Applications, 35, 7719
- Rue H., Martino S. and Chopin N. 2009, Journal of the Royal Statistical Society: Series B (Statistical Methodology), 71, 319
- Rue H., Riebler A., Sørbye S. H. et al. 2017, Annual Review of Statistics and Its Application, 4, 395
- Smole M., Rino-Silvestre J., González-Gaitán S., Stalevski M., 2022, A&A, 669, 152